Ca²⁺-induced inhibition of the cardiac Ca²⁺ channel depends on calmodulin

(heart/EF hand/IQ motif)

NING QIN*, RICCARDO OLCESE*, MICHAEL BRANSBY*, TONY LIN*, AND LUTZ BIRNBAUMER*†‡§¶‖

Departments of *Anesthesiology, †Biological Chemistry, and ‡Molecular, Cell and Developmental Biology, and §Brain Research, and ¶Molecular Biology Institutes, University of California, Los Angeles, CA 90095-1778

ABSTRACT Ca²⁺-induced inhibition of α_{1C} voltage-gated Ca²⁺ channels is a physiologically important regulatory mechanism that shortens the mean open time of these otherwise long-lasting high-voltage-activated channels. The mechanism of action of Ca²⁺ has been a matter of some controversy, as previous studies have proposed the involvement of a putative Ca²⁺-binding EF hand in the C terminus of α_{1C} and/or a sequence downstream from this EF-hand motif containing a putative calmodulin (CaM)-binding IQ motif. Previously, using site directed mutagenesis, we have shown that disruption of the EF-hand motif does not remove Ca²⁺ inhibition. We now show that the IQ motif binds CaM and that disruption of this binding activity prevents Ca²⁺ inhibition. We propose that Ca²⁺ entering through the voltage-gated pore binds to CaM and that the Ca/CaM complex is the mediator of Ca²⁺ inhibition.

Ca²⁺ entering through the cardiac voltage-gated Ca²⁺ channel is an essential event for the contraction of the heart muscle in response to a depolarizing stimulus. The opening of this channel is evident in the shape of the cardiac action potential and is responsible for the broad shoulder in its down stroke. The cardiac voltage-gated Ca²⁺ channel is of the long-lasting or L-type, showing only a minor voltage-induced inactivation component. Molecularly, it is made up of an α_1 subunit, α_{1C}, which is the pore-forming subunit proper, and β and $\alpha_2\delta$ regulatory or accessory subunits. The cardiac form of α_{1C} (1), which is expressed also in smooth muscle (2) and neurons (3), displays inhibition by incoming Ca²⁺ (4), although there are certain neuronal splice variants that are inhibited (5). In the heart, Ca²⁺-induced inhibition insures an inactivation rate compatible with the length of the Ca²⁺-mediated plateau phase in the action potential, which would be predicted to be much longer if inactivation proceeded according to the inactivation kinetics seen with Ba²⁺ as the charge carrier. This fact places Ca²⁺-induced inhibition of the cardiac Ca²⁺ channel at the center of the mechanisms that operate to insure coordinated contraction and relaxation cycles of the heart muscle fiber.

Kinetic arguments have placed the site of action of Ca²⁺ very close to the conduction pathway, but the location of this site has remained unknown and is subject to some controversy. de Leon *et al.* (6) focused on the existence of a Ca²⁺-binding consensus sequence, an EF hand, near the beginning of the 660-aa C-terminal tail of α_{1C} and tested for its participation in Ca²⁺ inhibition. They found that, although replacing the α_{1C} EF hand with a homologous but less perfect EF hand from the Ca²⁺-insensitive α_{1E} resulted in the loss of Ca²⁺ inhibition, the introduction into α_{1E} of a 250-aa α_{1C} segment, which included the 29-aa EF-hand motif, conferred Ca²⁺ sensitivity to the Ca²⁺-insensitive α_{1E}. This result led them to propose this motif as the site to which Ca²⁺ binds to inhibit channel activity. We analyzed α_{1E}/α_{1C} chimeras, as did de Leon *et al.* (6), but we subdivided the transferred segments further and were unable to substantiate their proposal. Instead, we pinpointed a shorter amino acid segment located downstream of the EF hand as essential for Ca²⁺ inhibition (7). This segment contains 144 aa and was designated RL–VS, denoting the beginning and ending amino acids. Experiments in which we tested for direct binding of ⁴⁵Ca²⁺ to the segment of α_{1C} that was able to confer Ca²⁺ sensitivity to α_{1E} were unsuccessful (N.Q. and L.B., unpublished results), leaving open the question as to how this segment conferred Ca²⁺ sensitivity to the channel and whether Ca²⁺ acted on the channel directly or indirectly.

Based on analysis of neuronal α_{1C} splice variants for their voltage- and Ca²⁺-dependent inactivation and on properties of artificial deletion mutants, Reuter and coworkers (5, 8) concluded that Ca²⁺-induced inhibition of α_{1C} depends on three amino acid sequences: (*i*) the EF-hand motif, (*ii*) two hydrophilic residues (N and E) 77–78 aa downstream of the EF hand, and, (*iii*) 40 aa downstream from these, an 8-aa sequence with an IQ motif. This last is a putative calmodulin (CaM)-binding motif located approximately in the middle of the RL–VS sequence. Zuehlke *et al.* (8) identified the three relevant sequences by the loss of function after their excision. In our previous studies, amino acid replacements within the EF-hand motif, which eliminated the motif but kept relative distances of the connected sequences undisturbed, preserved Ca²⁺ inhibition. This result led us to rule out the actual participation of the EF hand in Ca²⁺ inhibition. For this study, we directly tested the hypothesis that CaM binding to the IQ motif within the RL–VS sequence of α_{1C} mediates Ca²⁺ inhibition. Here, we report that indeed RL–VS binds the Ca/CaM complex, whereas fragments of α_{1C} without the IQ motif do not. Disruption of CaM binding by site-directed mutagenesis prevents Ca²⁺-mediated inhibition.

MATERIALS AND METHODS

Channel Expression in *Xenopus* Oocytes

The cDNAs encoding β_{2a}, $\alpha_2\delta$, and DN 60 (α_{1C} lacking amino acids 2–60), have been described (9–11), as have the methods for the preparation of cRNAs, the expression of these cRNAs in *Xenopus* oocytes, and the electrophysiological recording techniques (12–14).

Abbreviations: CaM, calmodulin; GSH, glutathione; GST, glutathione *S*-transferase.
‖To whom reprint requests should be addressed. e-mail: lutzb@ucla.edu.

Manipulation of cDNAs and Construction of Expression Vectors

The standard molecular-biology techniques that we (7, 11) and others (15) have described were used throughout. The nucleotide compositions of the final constructs were confirmed by double sequencing of double-stranded DNA by using the dideoxy chain-termination method (16).

Protein–Protein Interaction Tests

Glutathione *S*-Transferase (GST)-CaM Fusion Protein. The GST-CaM fusion plasmid was based on pGEX-4T-1 (Amersham Pharmacia) and was constructed by fusing the C terminus of GST to the N terminus of CaM. After transfection into *Escherichia coli* BL21, synthesis of the fusion protein was induced with 0.2 mM isopropyl β-D-thiogalactoside in a liquid culture grown to OD at 1.0 nm. After 2–3 h at 37°C, the cells were collected by centrifugation, resuspended in NETN lysis buffer (0.5% Nonidet P-40/1 mM EDTA/20 mM Tris·HCl, pH 8.0/100 mM NaCl; 1.0 ml of buffer per 20 ml of culture), and lysed by sonication. The lysate was cleared by centrifugation at $10,000 \times g$ for 10 min at 4°C. GST-CaM in the supernatant was adsorbed for 30 min at room temperature to Agarose-glutathione (GSH) beads (Amersham Pharmacia) [1 vol of lysate/1 vol of 50% (vol/vol) slurry of Agarose-GSH beads in NETN]. Finally, the beads were washed with binding buffer A (20 mM Tris·HCl, pH 7.5/100 mM NaCl/0.5% Triton X-100).

Synthesis of ^{35}S-Labeled α_{1C} Fragments by *in Vitro* Translation. ^{35}S-labelled forms of α_{1C} fragments having the compositions given in *Results* (see also Figs. 1–4) were synthesized with the TNT (transcription/translation) Coupled Rabbit Reticulocyte Lysate System (Promega) in the presence of [^{35}S]methionine following manufacturer's protocols. Aliquots of the incubation mixtures were used directly either for analysis by SDS/PAGE to confirm synthesis of proteins of the desired size or for the ability of the newly synthesized proteins to bind to GST or GST-CaM.

Protein–Protein Interactions. Slurries of Agarose-GSH beads [50% (vol/vol)] with ≈1 μg of GST or GST-CaM were incubated for 30 min at room temperature in a final volume of 200 μl of binding buffer A with 1 mM CaCl$_2$ and 10 μl of lysate that had been incubated with a template for the synthesis of α_{1C} fragments and contained 0.3–0.5 fmol of these fragments (the final concentration in the presence of GST or GST-CaM was 3–5 nM). At the end of the incubations, the beads were washed three times with 1.0 ml of binding buffer, resuspended in 15 μl of 2× Laemmli's sample buffer, and analyzed for retention by the GST-CaM fusion protein bound to Agarose-GSH with either a scintillation counter or by SDS/PAGE followed by autoradiography.

Calcium Buffering and Calculation of Free Ca^{2+} Ion

For incubations in which free Ca^{2+} was varied, Agarose-GSH::GST-CaM beads first were equilibrated in binding buffers with the desired concentrations of free Ca^{2+} ion, resuspended as a 50% (vol/vol) slurry, and then mixed with 1 volume of reticulocyte lysate incubates (40–60 nM α_{1C} C-terminal RL–VS peptide) and 18 volumes of binding buffer B (0.5% Triton X-100, 2.5 or 5.0 mM EGTA/CaCl$_2$ mixtures to give the indicated concentration of free Ca^{2+}, 100 mM NaCl, and 50 mM Bistris propane {1,3-bis[tris(hydroxymethyl)methylamino]propane, Sigma}, pH 7.0). The final pH was adjusted again to 7.0 with 1 M NaOH after adding the required amounts of CaCl$_2$. Free Ca^{2+} was calculated as described for free Mg^{2+} (17) by using the following equilibrium association constants: pK_a EGTA^{4-}·Ca^{2+}/CaEGTA^{2-} = 11.00 and pK_1 to pK_4 = 2.0, 2.68, 8.85, and 9.43, respectively (18). Taking into consideration that only EGTA^{4-} chelates Ca^{2+}, the corrected affinity constant of EGTA for Ca^{2+} at any given pH, $K_a'[pH]$ is calculated by applying the formula $K_a' = K_a/(1 + H/K_1 + H^2/K_1K_2 + H^3/K_1K_2K_3 + H^4/K_1K_2K_3K_4)$, where $-\log$ values of K_a and K_1 to K_4 were given above and H denotes the concentration of H$^+$. At pH 7.0, pK_a' for the EGTA–Ca^{2+} interaction is 6.91. This value corresponds to an equilibrium dissociation constant (K_d) of 123 nM. The affinity of EGTA for Ca^{2+} at pH 7.0 was validated experimentally by obtaining the same dependence on calculated free Ca^{2+} at two different total concentrations of EGTA (2.5 and 5.0 mM), requiring addition of different concentrations of CaCl$_2$ to obtain the same Ca^{2+}.

RESULTS

To test for the CaM-binding capacity of the IQ motif in RL–VS fragments of α_{1C}, we first attempted to prepare a GST-(RL–
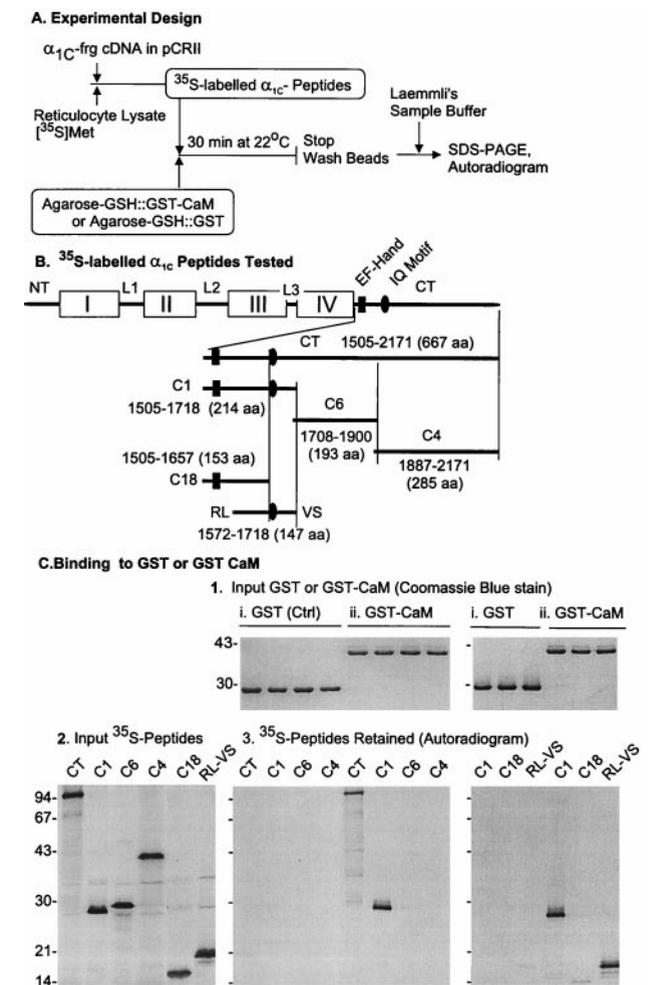
FIG. 1.   Identification of the RL–VS segment of the α_{1C} C terminus as an attachment site for CaM. (*A*) The strategy of the experiments. frg, fragment; [^{35}S]Met, [^{35}S]methionine. (*B*) Diagram of main structural motifs of α_{1C} and placement of C-terminal fragments in relation to each other. I–IV, homologous repeat sequences forming transmembrane domains of the Ca^{2+} channel; NT, N terminus; L1–L3, connecting loops; CT, C terminus. (*C*) Only RL–VS containing fragments of the C terminus bind CaM. Molecular mass markers are expressed in kDa. (*C*, 1) Input GST or GST-CaM visualized by Coomassie blue staining of polyacrylamide gels resulting from the electrophoresis of proteins eluted from Agarose-GSH::GST or GST-CaM that had been incubated with [^{35}S]α_{1C} fragments (partial view). (*C*, 2) Autoradiogram of SDS/PAGE analysis of *in vitro* translated α_{1C} fragments tested for CaM-binding activity. (*C*, 3) Autoradiogram of the gel shown in *C*, 1.
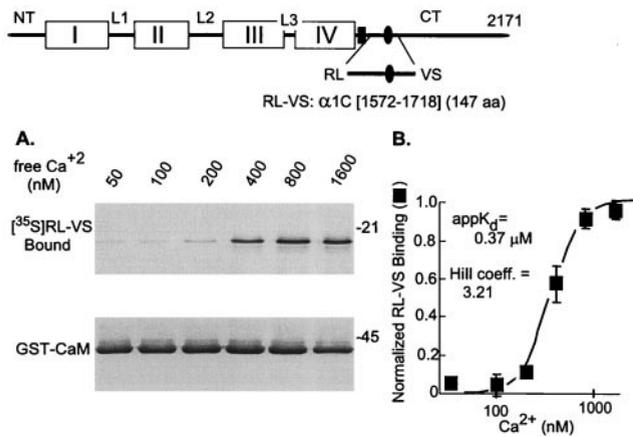
FIG. 2. Dependence of the CaM–(RL–VS) interaction on Ca^{2+}. (*Top*) Diagram depicting placement of RL–VS within the α_{1C} sequence. (*A*) Binding of $[^{35}S]$RL–VS (*Upper*) to GST-CaM (*Lower*). (*B*) Average of four experiments, two at 2.5 mM total EGTA and two at 5 mM total EGTA. For quantification, the $[^{35}S]$RL–VS bound to GST-CAM was counted in a liquid scintillation counter. Data were normalized to $[^{35}S]$RL–VS bound at 1.6 μM Ca^{2+}.

VS) fusion protein with the intention of adsorbing it to Agarose-GSH for incubation with CaM. However, we found that fusion proteins of proximal α_{1C} C-terminal fragments (i.e., fragments containing the first 200 aa after the last transmembrane segment of the channel), including GST-(RL–VS), are extremely insoluble under nondenaturing conditions. This fact made it impossible to study their CaM-binding activity. Therefore, we inverted the design of the experiment, fusing recombinant CaM to GST and testing whether GST-CaM would bind α_{1C} fragments made in radioactive form by *in vitro* translation in reticulocyte lysates in the presence of $[^{35}S]$methionine. Fig. 1 summarizes our findings, showing that although none of the α_{1C} C-terminal fragments bind to GST, the complete α_{1C} C terminus ($\alpha_{1C}[1,505–2,171]$) and fragments that contain the IQ motif bind to CaM. These fragments include RL–VS ($\alpha_{1C}[1,572–1,718]$). Fragments of the C terminus that did not harbor the IQ motif did not bind to GST-CaM. CaM binding was resistant to 500 mM KCl (data not shown).

CaM binding to α_{1C} fragments depended on not only the presence of the IQ motif in the peptide but also the concentration of Ca^{2+}. As determined with RL–VS, half-maximal binding was obtained at 0.37 μM (Fig. 2) and was highly

cooperative (Hill coefficient = 3.21). This result indicates that only CaM·Ca^{2+}_4 binds to the channel peptide.

These results suggested that CaM may mediate the inhibitory action of Ca^{2+} on α_{1C}. To substantiate this hypothesis, we mutated RL–VS to interfere with its CaM-binding activity and then tested whether loss of CaM binding would cause a functional correlate loss of Ca^{2+} inhibition. CaM binding was surprisingly resistant to amino acid substitutions in RL–VS. For example, changing IQ to AA, or IQEYFRK to AAAAAAA, had little if any effect (Fig. 2). CaM binding was reduced severely when IQEYF**RKFKKRK** was changed to IQEYF**EEFEEEE**, i.e., when a peptide in which the cluster of positively charged amino acids located after the IQ doublet was replaced with negatively charged amino acids (Fig. 3). Fig. 4 shows that loss of CaM binding led to a loss of inhibition of the channel by the incoming Ca^{2+}.

DISCUSSION

Previous structure-function studies with α_{1C} had pointed clearly to the proximal region of the C terminus as being important for Ca^{2+}-induced inhibition of this channel. This deduction was made both from deletion (excision) experiments and, to a lesser extent, from amino acid replacement experiments. Our previous deletion studies (7) together with those of Zuehlke and Reuter (8) have shown that although the presence of a peptide backbone chain is required in the place of the EF hand, a putative Ca^{2+}-binding function is not. It was determined that the region downstream of the EF hand is responsible for mediating Ca^{2+} inhibition by using a gain-of-function approach in which segments from the Ca^{2+}-sensitive α_{1C} were introduced into the Ca^{2+}-insensitive α_{1E} (7). The deletion mutants used by Zuehlke and Reuter (8) helped to narrow possible responsible amino acids to just a few, including a set that forms part of a consensus CaM-binding motif. We now have shown that the putative CaM-binding motif is real and that disruption of its CaM binding ability by amino acid replacement leads to loss of the inhibitory effect of Ca^{2+}.

The Ca^{2+} dependence for CaM binding is surprising, however. To account for Ca^{2+} inhibition of the channel, the dependence of CaM binding on Ca^{2+} suggests a reaction sequence in which Ca^{2+} enters through the pore, as suggested by the relation between the initial rate of inactivation and the activating voltage (4, 14), and then binds to CaM. CaM, in turn, on changing its conformation, would bind to the channel and initiate the intramolecular process that culminates in inactivation. Can the time in which the fluxing Ca^{2+} leads to
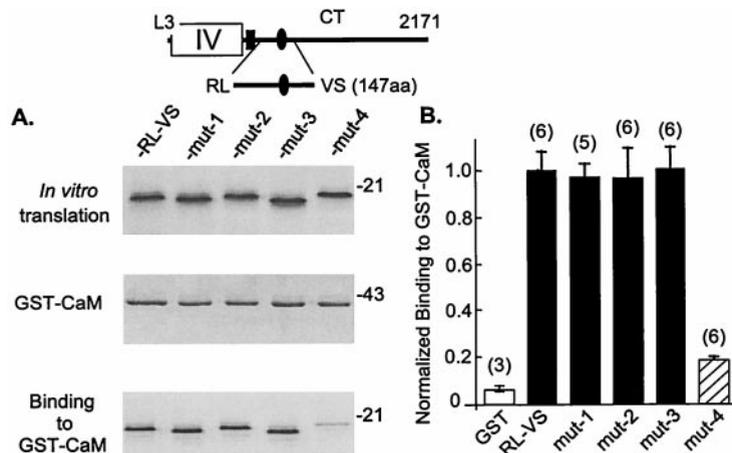
FIG. 3. Binding of RL–VS and mutant forms of RL–VS to GST-CaM. RL–VS ($\alpha_{1C}[1,572–1,718]$) contains $\alpha_{1C}[1,654$-IQEYFRKFKKRK-1,665]. mut-1, RL–VS with IQ → AA; mut-2, RL–VS with IQEYFR → IQEYF**E**; mut-3, RL–VS with IQEYFRK → **AAAAAAA**; mut-4, RL–VS with IQEYFRKFKKRK → IQEYF**EEFEEEE.** (*A*) Representative result. (*B*) Normalized binding to GST-CaM averaged from the number of experiments shown on top of the bars.
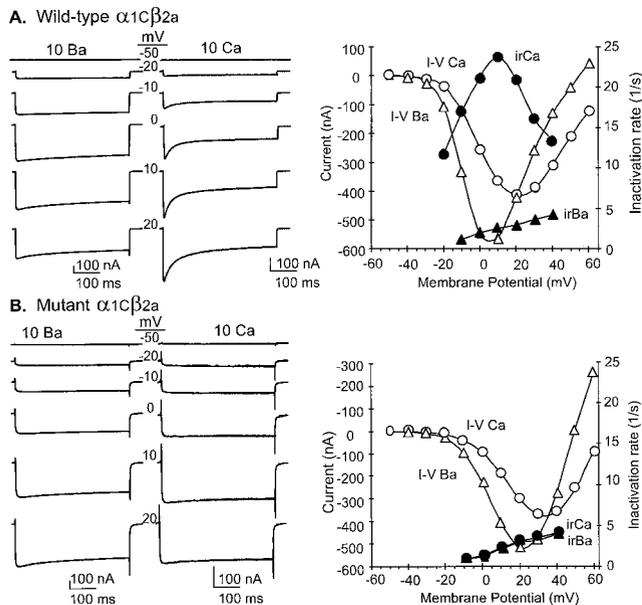
FIG. 4. Loss of Ca^{2+}-mediated inactivation in mutant α_{1C}, which is unable to bind CaM. β_{2a} and either wild-type α_{1C} (α_{1C}[1,654-**IQEYFRKFKKRK**-1,665]) or mutant α_{1C} (α_{1C}[1,654-**IQEY-FEEFEEEE**-1,665]) were coexpressed in *Xenopus* oocytes, and their activation and inactivation in the presence of either 10 mM Ca^{2+} or 10 mM Ba^{2+} as charge carriers were measured at the indicated test potentials. (*A*) Activation/inactivation time courses. Test potentials were set to the indicated voltages from a holding potential of −90 mM with either 10 mM Ba^{2+} or 10 mM Ca^{2+}. (*B*) Current–voltage (I–V) and inactivation rate–voltage (ir-V) relations. Peak current values and initial inactivation rates are shown as a function of test potentials. Time constants of inactivation in 10 mM Ba^{2+} were derived from fitting the decay phases of the time courses shown in *A* with a single-exponential decay function. The inactivation rate (irCa and irBa in the figure) is the inverse of the time constant of current decays. For wild-type $\alpha_{1C}\beta_{2a}$, the time constants in 10 mM Ca^{2+} were obtained from double-exponential fits. The fast component of inactivation was used for the inactivation rate. For mutant $\alpha_{1C}\beta_{2a}$, the time constants in 10 mM Ca^{2+} were obtained from single-exponential fits. For wild type, the results from a single representative oocyte are shown. For mutant α_{1C}, the means of seven oocytes from two frogs were averaged for both the 10 mM Ca^{2+} and the 10 mM Ba^{2+} conditions to give the I–V and inactivation rate–voltage relations shown. SEMs of inactivation rates were smaller than the symbols used to depict the inactivation rates on the figure. Error bars of I–V curves are not shown.

inactivation accommodate this multistep process that involves establishment of a protein–protein interaction? It is unlikely, given that Ca^{2+} inhibition is installed within the first millisecond of channel opening (14).

It follows that CaM binding to the channel should precede Ca^{2+} binding. Therefore, the CaM binding site uncovered in RL–VS should be "incomplete". The binding of CaM to larger fragments of the C terminus, including the complete 667-aa C-terminal fragment, was also Ca^{2+}-dependent. Thus, it would seem that in addition to the CaM-binding IQ motif of the C terminus identified here, there should exist one or more additional points of contact between the α_{1C} Ca^{2+} channel and CaM to enable CaM to become the constitutive Ca^{2+}-sensing

subunit. The possibility must be considered as well that the binding site identified here bears no relation to the site of action of Ca^{2+}, in spite of being a region of α_{1C} that confers Ca^{2+} sensitivity to the Ca^{2+}-insensitive α_{1E}. The present study should allow for a more focused design for future experiments dealing with the molecular basis of Ca^{2+} inhibition of the cardiac α_{1C} Ca^{2+} channel.

1. Mikami, A., Imoto, K., Tanabe, T., Niidome, T., Mori, Y., Takeshima, H., Narumiya, S. & Numa, S. (1989) *Nature (London)* **340,** 230–233.
2. Biel, M., Ruth, P., Bosse, E., Hullin, R., Stühmer, W., Flockerzi, V. & Hofmann, F. (1990) *FEBS Lett.* **269,** 409–412.
3. Snutch, T. P., Tomlinson, W. J., Leonard, J. P. & Gilbert, M. M. (1991) *Neuron* **7,** 45–57.
4. Neely, A., Olcese, R., Wei, X., Birnbaumer, L. & Stefani, E. (1994) *Biophys. J.* **66,** 1895–1903.
5. Soldatov, N. M., Zuehlke, R. D., Bouron, A. & Reuter, H. (1997) *J. Biol. Chem.* **272,** 3560–3566.
6. de Leon, M., Wang, Y., Jones, L., Perez-Reyes, E., Wei, X., Soong, T. W., Snutch, T. P. & Yue, D. T. (1995) *Science* **270,** 1502–1506.
7. Zhou, J., Olcese, R., Qin, N., Noceti, F., Birnbaumer, L. & Stefani, E. (1997) *Proc. Natl. Acad. Sci. USA* **94,** 2301–2305.
8. Zuehlke, R. D. & Reuter, H. (1998) *Proc. Natl. Acad. Sci. USA* **95,** 3287–3294.
9. Wei, X., Perez-Reyes, E., Lacerda, A. E., Schuster, G., Birnbaumer, L. & Brown, A. M. (1991) *J. Biol. Chem.* **266,** 21943–21947.
10. Wei, X., Neely, A., Olcese, R., Stefani, E. & Birnbaumer, L. (1996) *Recept. Channels* **4,** 205–215.
11. Qin, N., Platano, D., Olcese, R., Stefani, E. & Birnbaumer, L. (1997) *Proc. Natl. Acad. Sci. USA* **94,** 8866–8871.
12. Taglialatela, M. & Stefani, E. (1993) *Proc. Natl. Acad. Sci. USA* **90,** 4758–4762.
13. Noceti, F., Baldelli, P., Wei, X., Qin, N., Toro, L., Birnbaumer, L. & Stefani, E. (1996) *J. Gen. Physiol.* **108,** 143–155.
14. Noceti, F., Olcese, R., Qin, N., Zhou, J. & Stefani, E. (1998) *J. Gen. Physiol.* **111,** 463–475.
15. Sambrook, J., Fritsch, E. F. & Maniatis, T. (1989) *Molecular Cloning: A Laboratory Manual* (Cold Spring Harbor Lab. Press, Plainview, NY), 2nd Ed.
16. Sanger, F., Nicklen, S. & Coulson, A. B. (1977) *Proc. Natl. Acad. Sci. USA* **74,** 5463–5467.
17. Birnbaumer, L., Desmier, M., Stengel, D. & Hanoune, J. (1983) *Eur. J. Biochem.* **136,** 107–112.
18. Raaflaub, J. (1956) *Methods Biochem. Anal.* **3,** 301–324.
19. Xia, X.-M., Falker, B., Rivard, A., Wayman, G., Johnson-Pais, T., Keen, J. E., Ishil, T., Hirschberg, B., Bond, C. T., Lutsenko, S., *et al.* (1998) *Nature (London)* **395,** 503–507.